

Curing of carbon–fibre reinforced epoxy resin; non-invasive viscosity measurement by NMR imaging

P. JACKSON*

ICI plc, Wilton Materials Research Centre, PO Box 90, Wilton, Middlesbrough, Cleveland TS6 8JE, UK

Nuclear magnetic resonance (NMR) images have been obtained from small-scale samples (multi-laminate and rolled) made from a continuous carbon–fibre reinforced epoxy resin. Empirical relationships may be established between the image intensity observed and the internal viscosity of the polymer phase. Using slice-selective techniques, it is possible to obtain internal images, and hence measure local internal viscosity, non-invasively during the curing process. The results show that NMR imaging may be useful in optimizing both the processing conditions and performance of such materials by enabling the measurement of curing characteristics during manufacture.

1. Introduction

The rapidly expanding use of polymer composites in applications involving, for example, aerospace structures, industrial materials, tooling, automotive components and sporting goods, has led to an increasing requirement to be able to monitor polymeric materials, both during production and in service. With epoxy-based composites which are cured at elevated temperatures to form the required component, there is considerable interest in being able to monitor the cure state of the epoxy. The ability to perform such measurements during fabrication allows both the optimization of processing conditions, such as heating methods, pressures, temperatures and processing time-scales, and the design of novel chemical systems to make better use of time and energy to give more efficient and even curing across complex objects.

Nuclear magnetic resonance (NMR) imaging has recently been shown to be an excellent method by which to study the curing of methyl methacrylate, both at room temperature and at elevated temperatures (up to 60°C) [1, 2]. The results obtained allow spatially localized measurement of the residual monomer content (extent of reaction) as a function of time. High-temperature imaging is also valuable in the study of solvent ingress into polymers [3, 4] and in the direct imaging of solid materials above the glass transition temperature [5]. In addition, larger-scale room-temperature NMR imaging has proved valuable in the detection of voiding and delamination in solid carbon–fibre reinforced thermoplastic composite components by imaging the distribution of water ingress into the defects [6]. In order to investigate the applicability of high-temperature NMR imaging to the study of epoxy composite curing, several small-scale samples of a continuous carbon–fibre reinforced

epoxy resin have been imaged, with *in situ* curing at 90 and 100°C.

1.1. NMR imaging

NMR imaging is becoming increasingly familiar through the introduction of medical and biomedical scanners, enabling the replacement of more harmful X-ray investigations in many applications [7]. Imaging is generally performed with the most sensitive NMR nucleus, ^1H (protons). Medical images can be thought of as water distribution maps, with signals being picked up from the protons in the water in body tissues. In this work it is the protons in the epoxy resin that are imaged. Since the NMR frequency detected depends upon the strength of the applied magnetic field, application of a linear magnetic field gradient across a sample results in a distribution of NMR frequencies that can be related directly to spatial coordinates. The most common imaging technique used in materials science applications is Fourier imaging, where spatial information is encoded into refocused time-domain NMR signals (echoes) as both phase and frequency modulations (Fig. 1). The image is subsequently generated by Fourier transformation of the original NMR signals. By selectively switching orthogonal magnetic field gradients, images can be generated in one (profiles), two or three dimensions. In addition, modulated (shaped) excitation pulses combined with a magnetic field gradient allow thin planes through a sample to be selected for imaging.

The observation of NMR imaging signals depends crucially on the degree of molecular mobility present. In particular, the signal amplitude, S , observed depends on the spin–spin relaxation time, T_2 , which in turn is dependent on molecular mobility, as follows:

$$S \propto \exp(-t_e/T_2)$$

*Present address: ICI Specialities, Specialities Research Centre, PO Box 42, Hexagon House, Blackley, Manchester, M9 3DA, UK.

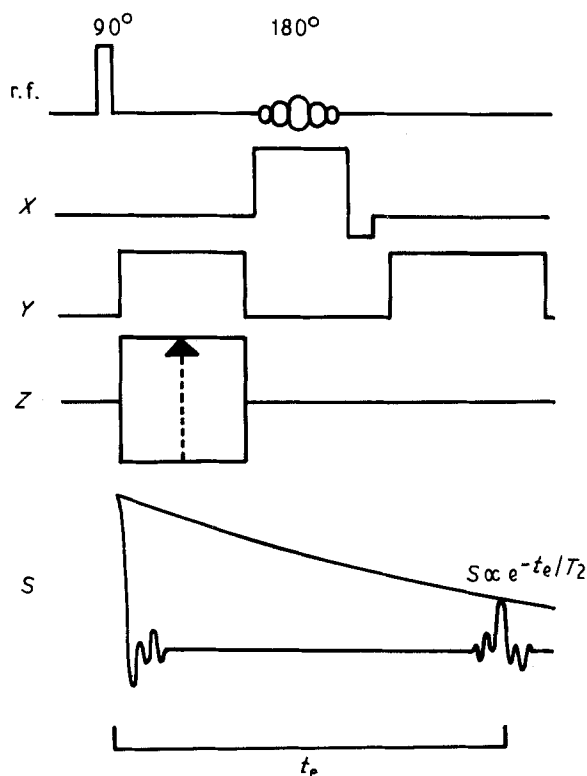


Figure 1 Radio-frequency pulse and field gradient timing sequence used to generate the images shown in this work. A thin slice through the sample is selected by use of the shaped (5-lobe sinc function) r.f. pulse in conjunction with the X gradient. The Y gradient is applied to provide frequency encoding of spatial information, whilst the Z gradient is stepped to phase-encode echo signals, which are recorded, building up a two-dimensional data matrix. The image is then obtained by two-dimensional Fourier transformation. The echo signal intensity, S , depends on the sample T_2 and the echo time, t_e .

where t_e is the experimental echo time. Conventional biomedical imaging spectrometers are generally limited to using echo times in excess of 20 ms, meaning that images can only be generated from materials with T_2 values greater than 10 ms. In liquids, T_2 values are generally in excess of 100 ms, allowing straightforward imaging, but rigid solids typically have T_2 values shorter than 100 μ s and cannot be imaged with such equipment. Systems configured for materials studies, however, should allow the use of echo times down to 1 ms, enabling the study of moderately rigid systems such as ingressed solvents, rubbers and viscous fluids. The advantage of operating at high temperatures in many materials applications is that molecular mobility is increased, leading to longer T_2 values and improved images [5]. This dependence of image signal on molecular mobility is exploited here to measure the cure state of an epoxy-based composite via changes in the polymer viscosity.

2. Experimental procedure

All work was performed using a Bruker MSL-200 NMR spectrometer configured for solid-state and mini-imaging studies and equipped with a 9.7 cm vertical-bore, 4.7 T magnet. The system operates at 200.13 MHz for ^1H observation. The probe-head used was home-made [8] and is capable of operation at temperatures up to 110 $^\circ\text{C}$. The sample coil was a simple horizontally-mounted solenoid, measuring 3 cm by 1.5 cm, giving an approximate homogeneous

region of 2 cm by 1 cm. Samples could be inserted and brought up to the desired temperature in less than 5 min, using the standard spectrometer variable temperature controller with dry nitrogen as the heating gas. Magnetic field gradients up to 10 G cm^{-1} were available in the X , Y and Z directions. A slice-selective sequence (Fig. 1) was employed to generate the images shown here, using an initial 3 μ s (hard) 90 $^\circ$ radio-frequency (r.f.) excitation pulse, followed by a 1 ms (soft, 5-lobe sinc function) 180 $^\circ$ refocusing pulse. The gradient values were adjusted to excite a 1 mm thick slice through the centre of the probe homogeneous region. A single echo time (5.00 ms) was used throughout, together with a recycle time of 0.5 s, allowing 128 \times 128 pixel images to be recorded in 64 s. Spin-spin relaxation, T_2 , measurements were made using identical imaging parameters, but recording echo signal amplitudes as a function of echo time. This means that the T_2 values obtained are directly relevant, allowing the calculation of expected image intensity for a given T_2 value and echo time.

All the work described was performed using ICI Fiberite 948A1, a continuous carbon-fibre reinforced epoxy resin. The material was stored below 5 $^\circ\text{C}$ (to slow down ageing) for one week before small sections were cut for imaging. A 20-ply sample was made up from 1.0 cm \times 0.7 cm sections, with fibres aligned orthogonally in adjacent plies. Rolled samples were made from a 1.0 cm wide strip, with the fibre direction parallel to the axis of the so-formed 1.0 cm diameter cylinder. The samples were held either between glass plates or inside a glass tube, depending on geometry, and positioned inside the imaging solenoid before being brought up to the temperature of interest.

3. Results

3.1. Image signal calibration

Using rolled samples, the temperature dependence of the epoxy T_2 was investigated. The results are shown in Fig. 2a. On raising the measurement temperature from 20 to 100 $^\circ\text{C}$, T_2 is found to increase from 160 μ s to 25.9 ms. By performing T_2 experiments in the first 5 min after reaching the appropriate temperature, it is possible to neglect the influence of reactive cross-linking on the results. During this early part of the cure cycle, the polymer viscosity is determined only by the temperature of the sample, and the increasing T_2 reflects the decreasing viscosity of the sample as the temperature is raised. Using an echo time of 5 ms, it is therefore possible to obtain images from the mobile epoxy at all temperatures above 55 $^\circ\text{C}$.

Fig. 2b shows a plot of polymer viscosity (log scale) versus temperature, obtained from the early part of a ramped temperature cure cycle described in the product data sheet [9]. Again, the contribution made by cross-linking to viscosity may be neglected during the early stage of the cure cycle. By combining the data in Fig. 2a and b, it is possible to arrive at a master curve relating the polymer T_2 to its viscosity. This is shown in Fig. 2c. Since the image signal observed depends on the echo time used and the T_2 of the polymer, it is now possible to develop further calibration curves for viscosity against image signal for each experimental echo

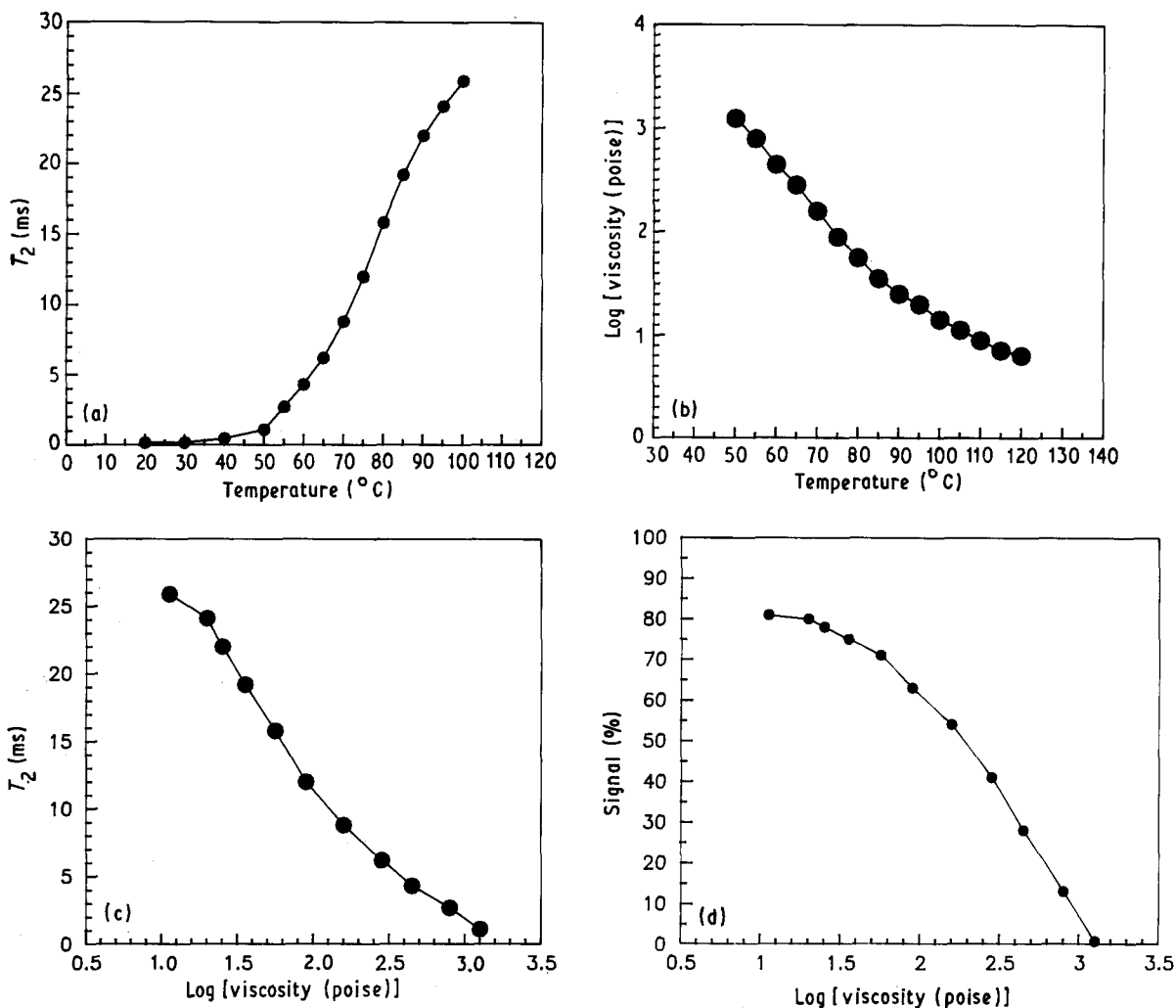


Figure 2 (a) Plot of epoxy T_2 versus temperature. (b) Plot of epoxy viscosity (log scale) versus temperature. From material data sheet [9]. (c) Master curve of T_2 against viscosity obtained by comparison of (a) and (b). (d) Derived plot of signal intensity versus viscosity using an echo time of 5.00 ms.

time used. The image signal is in terms of the percentage of the total available signal. Such a curve is illustrated in Fig. 2d for the echo time used in this work, 5.00 ms. These curves now enable

(a) the optimum imaging conditions to be used at a particular temperature, given the knowledge of T_2 values;

(b) the calibration of any temperature inhomogeneity across the sample during the early stages of a cure cycle by knowledge of the relationship between the image signal obtained at a particular location and the temperature; and

(c) the calibration of local viscosity changes within the sample due to cross-linking after thermal equilibrium has been reached by knowledge of the relationship between image signal and viscosity.

Thus it is possible to obtain images from the system which can give detailed information on important cure characteristics in a non-invasive, non-destructive fashion.

3.2. Multi-laminate sample

Fig. 3 shows images obtained at 40, 50, 60 and 70 °C from a 20-ply multi-laminate sample. These results

show, as expected from the T_2 measurements, that excellent images can be obtained at all temperatures above 55 °C, and that the image signal (brightness in this grey-scale representation) is extremely sensitive to temperature changes. The sample temperature was

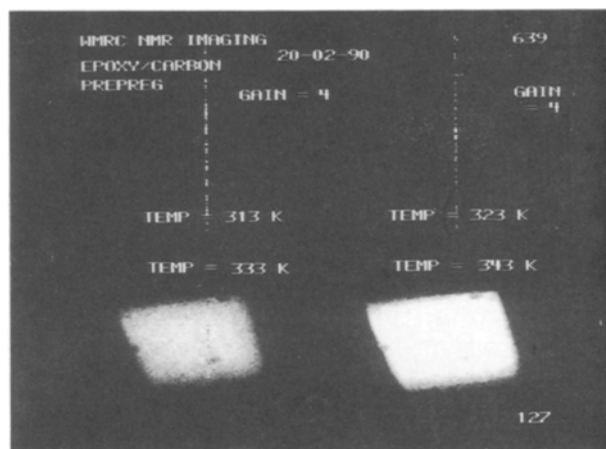


Figure 3 NMR images obtained from a 1.0 cm \times 0.7 cm, 20-ply sample at 40, 50, 60 and 70 °C (313, 323, 333 and 343 K). The image display gain has been increased by a factor of four for the upper two images. The central vertical line in some images is an experimental artefact.

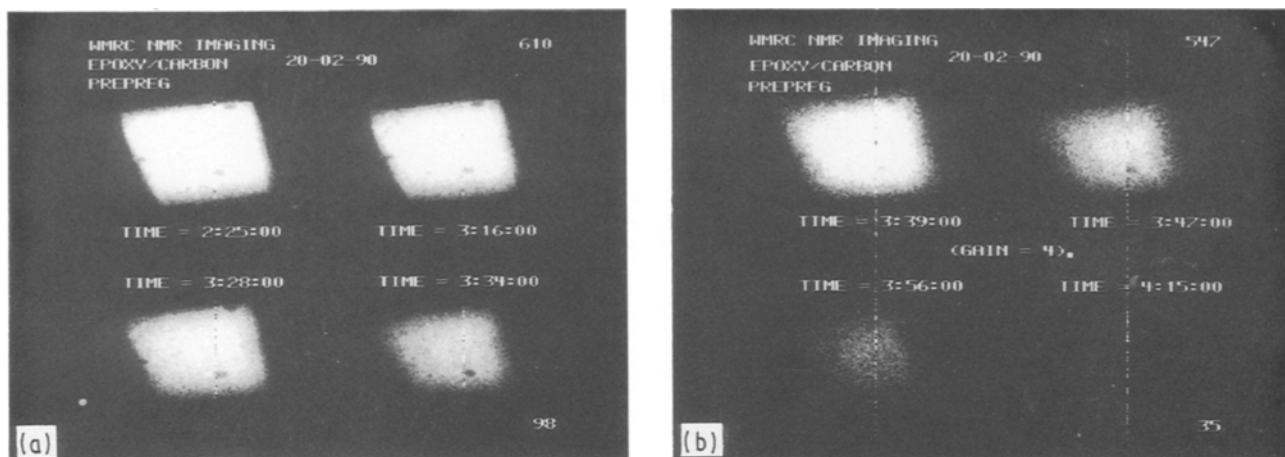


Figure 4 (a, b) NMR images obtained at 90°C as curing progresses. The times after initial insertion into the probe are indicated in h:min:s, though the actual time held at 90°C is much shorter. The image display gain has been increased by a factor of four in (b). Curing proceeds faster close to the block faces, as shown by the more rapid loss of intensity at the edge of the images.

increased in 10° steps from room temperature (20°C), taking 1 min per step, with 3 min allowed for equilibration before imaging. Three dark regions (top right, centre left and bottom centre) can be clearly seen in the images at 60 and 70°C. These correspond to air bubbles trapped between adjacent plies in the material. These would not be expected to be present under commercial fabrication conditions, but in this case illustrate the added potential of NMR imaging in defect detection in such systems.

After imaging at 70°C, the temperature was then increased to 90°C and images were recorded as a function of time, to observe the effect of the epoxy curing. Fig. 4 shows images obtained at the indicated times, showing the effect of increasing polymer viscosity. As cross-linking occurs, the viscosity increases, leading to a shorter T_2 and consequent diminishing image intensity. The lower four images are displayed with four times the image gain since the image signal is too low to show with the previous gain setting. As well as showing the effect of curing by the general loss of image intensity, the images also show that the curing reaction is anisotropic across the sample; the image signal diminishes first at the sample edges, rather than at the sample centre.

3.3. Rolled sample

In order to interpret images such as those in Figs 3 and 4 in terms of viscosity by means of the calibration curves described earlier, it is necessary, at some point, to measure the T_2 of the material in order to calibrate the image intensities. Once the T_2 and image signal magnitude are known, it is possible to define the maximum amount of signal available (i.e. the signal that would be observed at zero echo time). This value can then be used to scale the resulting images in percentage terms, or to back-calculate T_2 values from image intensities. This is best done in the early stages of the experiment, before significant cross-linking has occurred, allowing subsequent uninterrupted imaging of the curing process. This approach was demonstrated with a small rolled sample.

The sample was initially heated to 90°C and allowed to equilibrate for 10 min. A series of spin-echo signals was then recorded as a function of echo time, allowing the determination of the material T_2 . Images were then recorded every 2–4 min to follow the progression of the curing process. The results are shown in Fig. 5. The time after thermal equilibration is indicated below each image. The lower series of images, with low intensity after 60 min, is displayed with double the image display gain. The results were as expected for a system with viscosity increasing as cross-linking proceeds. After 90 min no further images could be obtained since T_2 had fallen to too low a value. In this case there was a spatially more even disappearance of signal, indicating a more uniform curing of the polymer through the sample.

The image intensity was measured in a 4 × 4 pixel region in each case, and the results are plotted in Fig. 6a. The image signals have been converted to percentage values of the total available signal. It is now possible to convert image signal values directly to viscosity, using the master curves outlined in section 3.1. The results of this process are shown in Fig. 6b, where localized image signal intensity has now been converted to viscosity. The internal viscosity of the polymer is seen to rise continuously during the time course of the experiment, from 10 poise after 6 min to 3200 poise after 90 min, defining the cure characteristics under these particular “processing” conditions.

4. Conclusions

These preliminary results show the great potential of NMR imaging in the study of the curing of epoxy systems. It is straightforward to obtain, non-invasively, viscosity information from images by a suitable calibration scheme. It should also be relatively straightforward to incorporate the relevant calibration curves into image processing and display software, enabling maps of viscosity, rather than NMR signal images, to be produced. The maximum viscosity accessible to the imaging experiment is currently limited by the length of the echo time used. By

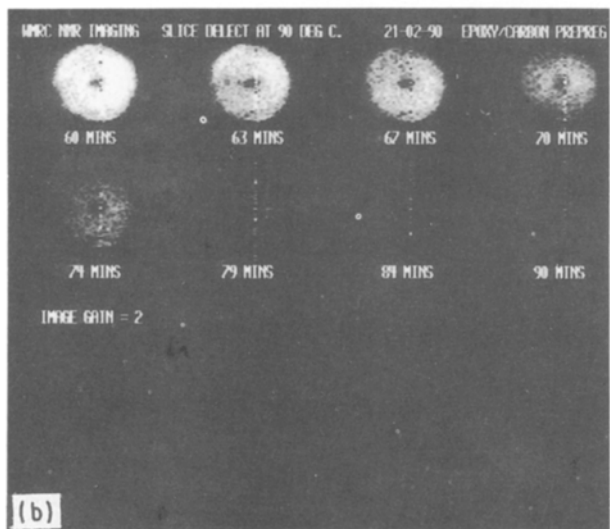
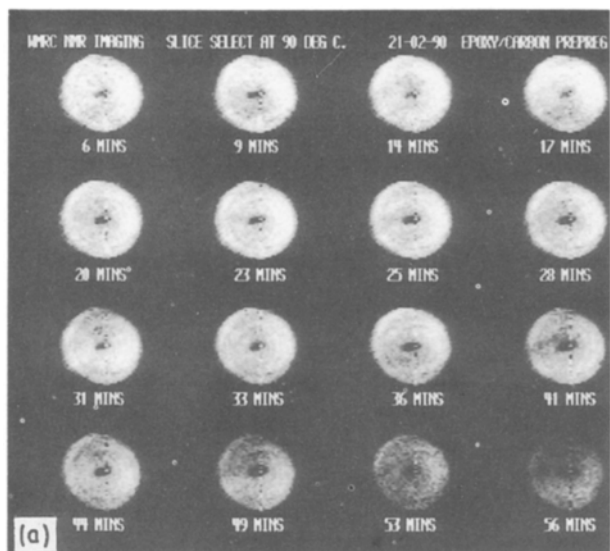


Figure 5 (a, b) NMR images obtained from a rolled sample at 90 °C as a function of cure time. The times after reaching the set temperature are indicated. The image display gain has been increased by a factor of two in (b).

performing experiments at shorter echo times, it should be possible to measure internal viscosities in excess of 2000 poise. The use of more rapid imaging schemes would enable much faster curing mechanisms to be investigated, offering the potential to obtain images in less than 1 s.

Whilst the samples here were subjected to only modest temperatures, it is hoped to develop further the principles outlined in this paper to include the analysis of test samples produced under conditions approaching those found in commercial processing facilities. This will include the use of temperatures up to 200 °C, and of pressures up to 5 kg cm⁻². It is also hoped to increase the size of samples studied up to approximately 20 cm × 10 cm × 0.5 cm by using wide-bore magnet technology. Such an increase in sample size will allow the mechanical properties of test samples to be investigated following on from imaging during production. In this way, NMR imaging may help to optimize both the processing conditions and the polymer chemistry to give the required end-use material properties.

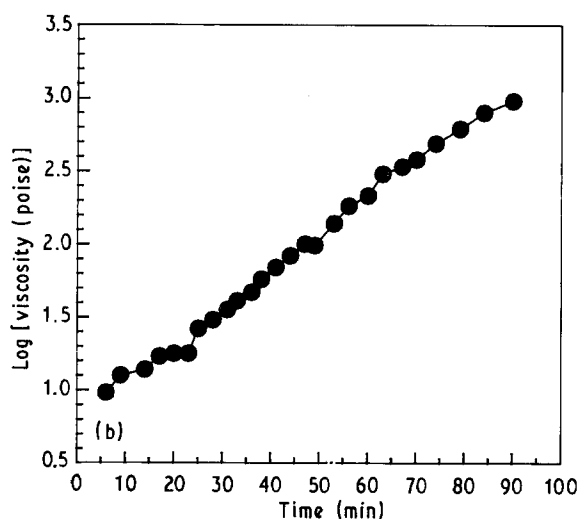
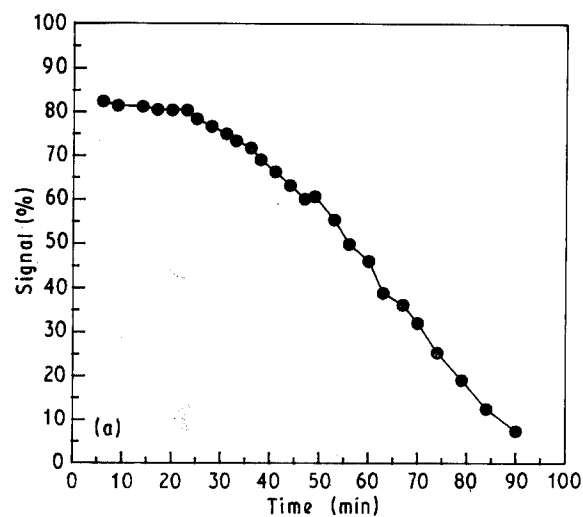


Figure 6 (a) Plot of image signal versus curing time obtained from the images in Fig. 5. (b) Derived plot of internal viscosity versus curing time obtained by calibration of (a) with the curve shown in Fig. 2d.

Acknowledgements

The author would like to thank Dr M. Commander (ICI) for the sample materials used in this work.

References

1. P. JACKSON, N. J. CLAYDEN, N. J. WALTON, T. A. CARPENTER, L. D. HALL and P. JEZZARD, *Polym. Int.* **24** (1991) 139.
2. P. JACKSON, N. J. CLAYDEN, N. J. WALTON, T. A. CARPENTER, L. D. HALL, P. JEZZARD and C. WIGGINS, poster C.7, 10th European Experimental NMR Conference, Veldhoven, 1990.
3. S. BLACKBAND and P. MANSFIELD, *J. Phys. C. Solid State Phys.* **19** (1986) L49.
4. P. JACKSON, *J. Adhesion* **33** (1990) 1.
5. P. JEZZARD, T. A. CARPENTER, L. D. HALL, P. JACKSON and N. J. CLAYDEN, *Polym. Commun.* in press.
6. P. JACKSON, J. A. BARNES, N. J. CLAYDEN, T. A. CARPENTER, L. D. HALL and P. JEZZARD, *J. Mater. Sci. Lett.* **9** (1990) 1165.
7. P. G. MORRIS, "Nuclear Magnetic Resonance Imaging in Medicine and Biology" (Oxford University Press, New York, 1986).
8. P. JEZZARD, L. D. HALL, T. A. CARPENTER, P. JACKSON and N. J. CLAYDEN, *Polym. Commun.* in press.
9. ICI Fiberite data sheet, 948A1 Epoxy Resin (1989).

Received 16 January
and accepted 7 June 1991